RESEARCH ARTICLE

Analysis of the mRNA Targetome of MicroRNAs Expressed by Marek's Disease Virus

Oren Parnas,[a] David L. Corcoran,[b] Bryan R. Cullen[a]

Department of Molecular Genetics & Microbiology and Center for Virology, Duke University Medical Center, Durham, North Carolina, USA[a]; Institute for Genome Sciences and Policy, Duke University, Durham, North Carolina, USA[b]

ABSTRACT   Marek's disease virus 1 (MDV-1), an oncogenic α-herpesvirus that induces T-cell lymphomas in chickens, serves as model system to study transformation by lymphotropic herpesviruses. Like the oncogenic human γ-herpesviruses Kaposi's sarcoma-associated herpesvirus (KSHV) and Epstein-Barr virus (EBV), MDV-1 encodes several viral microRNAs (miRNAs). One MDV-1 miRNA, miR-M4, shares the same "seed" targeting sequence with both a KSHV miRNA, miR-K11, and cellular miR-155. Importantly, miR-M4 plays a critical role in T-cell transformation by MDV-1, while miR-K11 and cellular miR-155 are thought to play key roles in B-cell transformation by KSHV and EBV, respectively. Here, we present an analysis of the mRNAs targeted by viral miRNAs expressed in the chicken T-cell line MSB1, which is naturally coinfected with MDV-1 and the related nonpathogenic virus MDV-2. Our analysis identified >1,000 endogenous mRNAs targeted by miRNAs encoded by each virus, many of which are targeted by both MDV-1 and MDV-2 miRNAs. We present a functional analysis of an MDV-1 gene, RLORF8, targeted by four MDV-1 miRNAs and a cellular gene, encoding interleukin-18 (IL-18) and targeted by both MDV-1 and MDV-2 miRNAs, and show that ectopic expression of either protein in a form resistant to miRNA inhibition results in inhibition of cell proliferation. Finally, we present a restricted list of 9 genes targeted by not only MDV-1 miR-M4 but also KSHV miR-K11 and human miR-155. Given the critical role played by miR-155 seed family members in lymphomagenesis in humans and chickens, these mRNA targets may contain genes whose inhibition plays a conserved role in herpesvirus transformation.

IMPORTANCE   Herpesviruses cause lymphomas in both humans and chickens, and in both cases, evidence indicates that virally encoded miRNAs, or virally subverted cellular miRNAs, belonging to the miR-155 seed family, play a critical role in this process. However, because each miRNA regulates numerous cellular mRNAs species, it has been difficult to elucidate which miRNA targets are important. Given the evolutionary distance between chickens and humans and the observation that miR-155 is nevertheless highly conserved in both species, we reasoned that the identification of shared miR-155 targets might shed light on this process. Here, we present an analysis of the mRNAs targeted by miRNAs encoded by the oncogenic avian herpesvirus MDV-1 in transformed chicken T cells, including a short list of mRNAs that are also targeted by miR-155 seed family miRNAs in EBV- or KSHV-transformed human B cells, and present an initial functional analysis of some of these miRNA targets.

MicroRNAs (miRNAs) are small, ~22-nucleotide (nt) regulatory RNAs that can downregulate the expression of mRNAs bearing complementary target sequences (1). miRNAs are initially transcribed in the nucleus as long primary miRNA (pri-miRNA) precursors that contain one or several miRNAs embedded in the stems of imperfect, ~80-nt-long stem-loop structures. These stem-loops are targets for the nuclear RNase III enzyme Drosha, which cleaves the stem ~22 bp from the terminal loop to liberate an ~60-nt hairpin RNA called a pre-miRNA intermediate (2). After export to the cytoplasm (3), the pre-miRNA is cleaved by a second RNase III enzyme, Dicer, to liberate the ~22-bp miRNA duplex intermediate (4). One strand of this duplex then associates with a cellular Argonaute (Ago) protein to generate the RNA-induced silencing complex RISC (1). While one strand of the miRNA duplex intermediate is generally strongly favored for in-

corporation into RISC, with the other strand being degraded, this discrimination is rarely complete, and potentially significant levels of the other strand, referred to as the miRNA passenger or star strand, can often be detected (5). Once incorporated into RISC, the miRNA acts as a guide RNA to target RISC to mRNAs bearing partially or fully complementary target sites, resulting in their translation inhibition and/or degradation (1). Functional miRNA target sites are generally located in the mRNA 3′ untranslated region (UTR), and while miRNA homology to the target site does not need to be extensive, full complementarity to nucleotides 2 to 7 or 8 of the miRNA, referred to as the miRNA seed region, is generally required for effective downregulation (1).

Analysis of the potential of viruses to express miRNAs has shown that almost all herpesviruses of humans and animals encode multiple viral miRNAs that play a role in downregulating

cellular mRNAs, often encoding factors with antiviral potential, as well as in some cases regulating the expression of viral mRNAs, including mRNAs encoding factors involved in the latent-to-lytic transition of viral infections (6–9). Chickens are subject to infection by two members of the *Mardivirus* genus of avian α-herpesviruses, Marek's disease virus type 1 (MDV-1) and MDV-2 (10). MDV-1 causes an economically important poultry disease (11) and induces rapid-onset T-cell lymphomas within weeks of infection of susceptible chickens (12). In contrast, the related virus MDV-2 is nonpathogenic and is widely used as a vaccine to prevent disease caused by MDV-1. MDV-1 and MDV-2 have previously been reported to encode 13 and 18 distinct pre-miRNAs, respectively, that give rise to numerous miRNAs and miRNA passenger strands, with some of the latter being expressed at substantial levels (13–18). However, little is known about the mRNAs targeted by these viral miRNAs, although some mRNAs are encoded antisense to viral coding sequences and therefore clearly have the potential to restrict the expression of specific viral proteins (18). One MDV-1 miRNA that has drawn significant attention is miR-M4, as it has the same seed sequence as both the cellular miRNA miR-155 (17, 19), conserved in both humans and chickens, and another viral miRNA, miR-K11, expressed by the oncogenic human γ-herpesvirus Kaposi's sarcoma-associated virus (KSHV) (20, 21). Importantly, previous work has clearly demonstrated that KSHV miR-K11 and human miR-155 can indeed target very similar populations of cellular mRNAs (20, 21) and that miR-K11 can even substitute for miR-155 in promoting the normal development of B cells *in vivo* (22, 23).

While miR-155 is required for normal function of lymphoid cells, inappropriate expression is associated with B- and T-cell lymphoma development (24). Moreover, while for technical reasons it remains unclear whether miR-K11 promotes oncogenesis by KSHV, it is known that B-cell transformation by Epstein-Barr virus (EBV), a second oncogenic human γ-herpesvirus, requires the massive transcriptional upregulation of cellular miR-155 expression (25, 26), presumably to compensate for the fact that EBV, unlike KSHV, does not encode a miR-155 analog. Finally, analysis of miR-M4 function has shown that MDV-1 mutants lacking miR-M4 are severely attenuated in their ability to induce T-cell lymphomas in chickens, even though viral replication *per se* was largely unaffected (27). Therefore, these data indicate that transformation of B cells by human γ-herpesviruses, and transformation of T cells by MDV-1, requires the downregulation of one or more cellular mRNA species by a miR-155 seed family miRNA. As chicken and human miR-155 are essentially identical, we hypothesize that the same key cellular mRNAs are involved in transformation by EBV, KSHV, and MDV-1.

Previously, we sought to identify mRNA targets for KSHV miR-K11 and human miR-155 by photoactivatable ribonucleoside-enhanced cross-linking and immunoprecipitation (PAR-CLIP) analysis of RISC binding sites in KSHV- or EBV-transformed human B-cell lines (28, 29), and similar studies have also been performed in latently KSHV- or EBV-infected B cells using the similar HITS-CLIP (high-throughput sequencing of RNA isolated by CLIP) technology (30, 31). PAR-CLIP and HITS-CLIP are techniques that allow the recovery of RISC binding sites by inducing cross-linking of mRNAs to bound RISC by UV irradiation followed by recovery, reverse transcription, and deep sequencing of these RNA binding sites (28–33). The millions of reads obtained are then bioinformatically analyzed (34), to iden-

tify RISC binding clusters on mRNAs and to assign the miRNA that has guided RISC to that cluster. Using this approach, we were previously able to identify ~500 mRNAs targeted by miR-155 and ~410 mRNAs targeted by miR-K11 (28, 29), of which at least 231 were targeted by both miRNA species. However, this is still an unwieldy number. We therefore were interested in whether analysis of miR-M4 target sites in an MDV-1-infected chicken T-cell lymphoma would identify a smaller number of mRNAs that are targeted not only by miR-155 and miR-K11 in human cells but also by miR-M4 in chicken cells. As chicken mRNA 3′ UTRs are generally quite divergent from human mRNA 3′ UTRs, this seemed likely to be the case.

In this article, we present an analysis of the expression and mRNA targetome of MDV-1 and MDV-2 miRNAs present in the chicken T-cell lymphoma cell line MSB1 (15, 35), which is naturally coinfected by MDV-1 and MDV-2. We did not identify any novel MDV-1 or MDV-2 pre-miRNAs but did confirm the existence of the previously reported 13 MDV-1 and 18 MDV-2 pre-miRNAs (13–18). Interestingly, we demonstrate that three MDV-1 miRNAs and 4 MDV-2 miRNAs exist in two isoforms that differ by one or two nucleotides at their 5′ ends. This gives rise to two different seed sequences, and we demonstrate that each of these six viral miRNAs actually targets two overlapping but distinct sets of cellular mRNAs. Moreover, MDV-1 miR-M9-5p has the same seed sequence as the longer isoform of MDV-2, miR-M28-5p, which represents the first demonstration that MDV-1 and MDV-2 miRNAs have the potential to target some of the same sites on mRNAs. Indeed, PAR-CLIP analysis of the 3′ UTRs of cellular mRNAs bound by MDV-1 and MDV-2 miRNAs shows that these extensively overlap, albeit in most cases at distinct sites.

In terms of target identification, our data confirm that MDV-1 miR-M4, miR-M2, miR-M3, and miR-M12, located antisense to the viral RLORF8 gene, indeed restrict RLORF8 expression and demonstrate that ectopic RLORF8 expression, in a form resistant to miRNA inhibition, is toxic for MSB1 cells. We also identify the chicken interleukin-18 (IL-18) mRNA 3′ UTR as a target for two MDV-1 and five MDV-2 miRNAs and show that ectopic expression of IL-18 in a form lacking its 3′ UTR is also inhibitory for MSB1 cell growth. Finally, we identify a restricted set of nine mRNA 3′ UTRs targeted not only by miR-155 and miR-K11 in human B cells but also by miR-M4 in chicken T cells and demonstrate that these mRNAs are indeed susceptible to inhibition by both miR-155 and miR-M4. This will hopefully inform and facilitate our ongoing efforts to define the mRNA targets for miR-K11 and miR-155 that are important for lymphomagenesis in humans.

RESULTS

Analysis of the MDV-1 and MDV-2 microRNA expression profile. Conventional and deep sequencing analyses of the viral miRNAs expressed by MDV-1 and MDV-2 have previously identified 13 pre-miRNAs encoded by MDV-1 and 18 pre-miRNAs encoded by MDV-2 (13–18). While these miRNAs are derived from analogous regions of the viral genome, this work did not identify any MDV-1 and MDV-2 miRNAs with the same seed sequence and hence the potential to target a similar set of mRNA transcripts.

We performed deep sequencing of small, ~18- to 25-nt-long RNAs expressed in MSB1 cells, a chicken lymphoblastoid cell line previously shown to be naturally infected by both MDV-1 and MDV-2 (14, 15). This generated 186,022,013 reads, of which 184,005,445 could be aligned to either the chicken genome or the

MDV-1 or MDV-2 genome. Of these, 161,068,074 (88%) aligned to known chicken, MDV-1, or MDV-2 pre-miRNAs, as listed in miRBase version 19. Reads aligning to known chicken miRNAs contributed 49% of the total miRNAs detected, while MDV-1 and MDV-2 contributed 42% and 9%, respectively (Fig. 1A). The most highly expressed single miRNA, chicken miR-21, contributed ~22% of all miRNAs detected, followed by MDV-1 miR-M4 (10%), MDV-1 miR-M3 (10%), chicken miR-142 (7%), and MDV-1 miR-M1 (6%) (Fig. 1B). The most highly expressed MDV-2 miRNA, miR-M29, contributed 4% of all miRNA reads.

Analysis of all small RNA reads that mapped to the MDV-1 or MDV-2 genome failed to identify any novel viral miRNAs and confirmed the expression of miRNAs and, in most cases, miRNA passenger strands derived from all of the 13 previously reported MDV-1 pre-miRNAs and 18 MDV-2 pre-miRNAs (13–18). The major isoforms of the MDV miRNAs and miRNA passenger strands derived from these 31 pre-miRNA precursors are listed in Tables 1 and 2. Given the key role played by the miRNA seed region (1), nucleotides 2 through 8, in mRNA target identification, we were not surprised to find that viral miRNA sequence variation was primarily restricted to the 3′ end, which plays a less important role in target selection. However, we did note several viral miRNAs that were processed into two different miRNA species that differed at their 5′ ends and therefore would be predicted to target overlapping but distinct mRNA populations. These included MDV-1 miR-M3-5p, where a 5′ end variant of the dominant miRNA provided 16% of all reads, as well as MDV-1 miR-M7-5p (38%), and miR-M12-3p (10%) (Table 1). In MDV-2, major 5′ variants were detected for miR-14-5p (31%), miR-M18-5p (14%), miR-M24-3p (13%), and miR-M28-5p (29%) (Table 2). To confirm that viral miRNAs are indeed expressed in two major isoforms that differ at their 5′ ends, we performed primer extension analysis for several of these viral miRNAs. These data confirmed the existence of two isoforms of MDV-1 miR-M3-5p and miR-M7-5p, as well as MDV-2 miR-M18-5p, that differ by 1 nt and two isoforms of MDV-2 miR-M28-5p that differ by 2 nt at their 5′ ends (Fig. 1C). Interestingly, the novel, extended isoform of MDV-2 miR-28-5p has the same predicted seed sequence as MDV-1 miR-M9-5p (Fig. 1D), and this therefore represents the first example of an MDV-1 and MDV-2 miRNA pair with the same seed sequence and hence, presumably, a similar mRNA target population.

The mRNA targetome of MDV microRNAs. Having identified all viral miRNA species expressed in the MSB1 lymphoblastoid cell line, we next sought to identify the cellular and viral mRNA populations targeted by these miRNAs using the previously described photoactivatable ribonucleoside-enhanced cross-linking and immunoprecipitation (PAR-CLIP) procedure (28, 29, 32). For this purpose, MSB1 transcripts were labeled by growth of cells in 4-thiouridine, followed by cross-linking of RNAs to bound proteins by irradiation at 365 nm. After lysis, RNA fragments bound to RISC were isolated by immunoprecipitation using a pan-Ago antibody followed by RNase treatment, linker ligation, reverse transcription, PCR amplification, and deep sequencing. Analysis of the PAR-CLIP reads obtained, using the previously described PARalyzer software (34), identified 16,585 RISC-binding clusters which mapped primarily to mRNA coding regions, 3′ UTRs, and intergenic regions (Fig. 2A). (Note that the chicken transcriptome is currently not well defined, so intergenic regions are expected to be overrepresented.) A list of all RISC
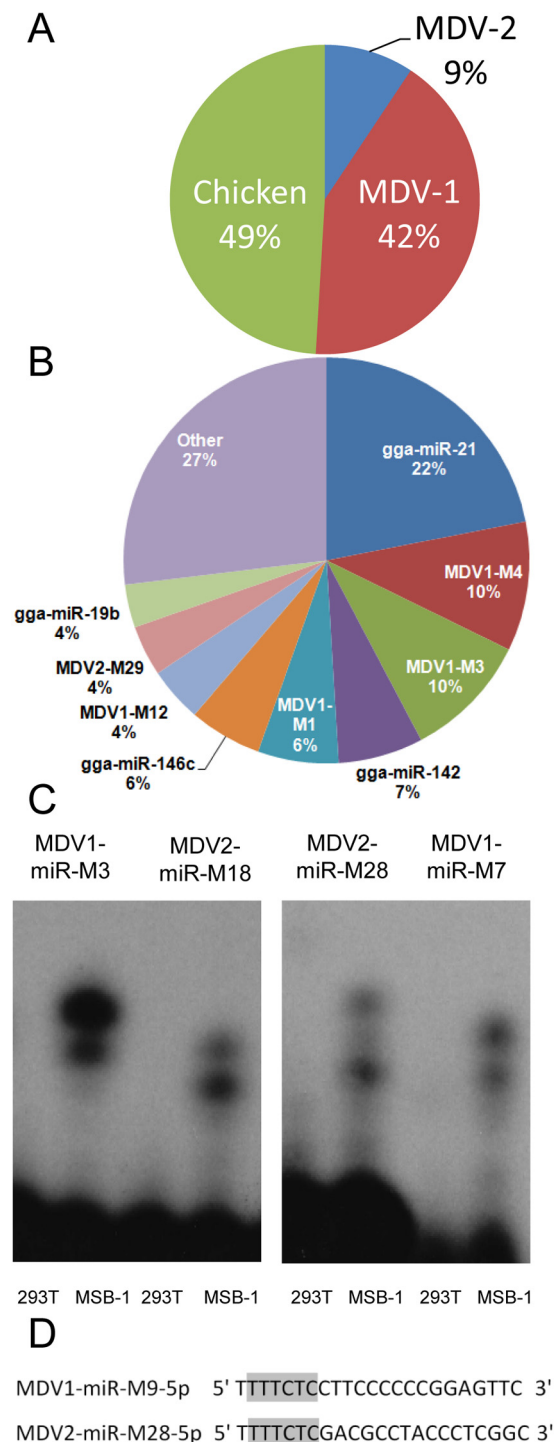

FIG 1 Analysis of the small-RNA library generated from MSB1 cells. (A) Cellular and viral distribution of observed miRNAs. (B) The most abundant chicken, MDV-1, and MDV-2 miRNAs present in MSB1 cells are indicated. (C) Primer extension analysis of four viral miRNAs that show predicted 5'-end variation. This experiment was performed using total RNA from MSB1 cells. Total RNA from MDV-negative 293T cells was used as a control. (D) These MDV-1 and MDV-2 miRNAs share the same seed sequence.

binding clusters identified, with their predicted miRNAs, is given in Table S1 in the supplemental material. Of these 16,585 binding

TABLE 1 MDV-1 miRNAs expressed in MSB-1 cells[a]

miRNA	Sequence	Length	Position Beginning	End	Frequency	%
MDV1-M1-5p	TGCTTGTTCACTGTGCGGCATT	22	4725	4746	5,220,661	51
	TGCTTGTTCACTGTGCGGCATTA	23	4724	4746	3,483,446	34
MDV1-M1-3p	ATGCTGCGCATGAAAGAGCGA	21	4687	4707	38,270	68
MDV1-M2-5p	GTTGTATTCTGCCCGGTAGTCCGT	24	7365	7388	773,504	43
	GTTGTATTCTGCCCGGTAGTCCGTT	25	7364	7388	420,366	24
	GTTGTATTCTGCCCGGTAGTCCG	23	7366	7388	291,031	16
MDV1-M2-3p	CGGACTGCCGCAGAATAGCTT	21	7328	7348	285,919	56
MDV1-M3-5p	ATGAAAATGTGAAACCTCTCCCGC	24	7516	7539	8,707,716	54
	TGAAAATGTGAAACCTCTCCCGC	23	7516	7538	2,554,622	16
MDV1-M3-3p	TGGGGGGTTCACATTTTTAAGT	22	7479	7500	129	70
MDV1-M4-5p	TTAATGCTGTATCGGAACCCTTCGT	25	7227	7251	7,837,697	47
	TTAATGCTGTATCGGAACCCTTCG	24	7228	7251	4,059,588	25
	TTAATGCTGTATCGGAACCCTTC	23	7229	7251	2,754,899	17
MDV1-M4-3p	AATGGTTCTGACAGCATGACC	21	7194	7214	42,714	40
MDV1-M5-5p	CGTATGCGATCACATTGACACG	22	7990	8011	867	57
MDV1-M5-3p	TGTGTATCGTGGTCGTCTACTGT	23	7950	7972	1,069,623	84
MDV1-M6-5p	TGTTGTTCCGTAGTGTTCTCG	21	176086	176106	3,255,817	65
	TGTTGTTCCGTAGTGTTCTCGT	22	176085	176106	1,045,694	21
MDV1-M6-3p	AGATCCCTGCGAAATGACAGT	21	176053	176073	76,487	77
MDV1-M7-5p	GTTATCTCGGGGAGATCTCGAT	22	175913	175934	1,527,552	39
	TGTTATCTCGGGGAGATCTCGA	22	175914	175935	1,490,315	38
	GTTATCTCGGGGAGATCTCGA	21	175914	175934	523,225	13
MDV1-M7-3p	GAGATCTCTACGAGATTACAGT	22	175874	175895	26,918	43
MDV1-M8-5p	TATTGTTCTGTGGTTGGTTTCGA	23	176205	176227	346,016	51
MDV1-M8-3p	TGACCTCTACGGAACAATAGT	21	176206	176227	803,339	71
	TGACCTCTACGGAACAATAGC	21	176164	176184	126,023	11
MDV1-M9-5p	TTTTCTCCTTCCCCCCGGAGTTC	23	8223	8245	564,957	72
MDV1-M9-3p	AAACTCCGAGGGCAGGAAAAAG	22	8184	8205	13,504	51
MDV1-M10-5p	GCGTTGTCTCGTAGAGGTCCCGA	23	175795	175817	11,127	51
MDV1-M10-3p	GAAATCTCTACGAGATAACAGT	22	175753	175774	1,290,839	86
MDV1-M11-5p	TTTTCCTTACCGTGTAGCTTAGA	23	5544	5566	16,899	80
	TTTTCCTTACCGTGTAGCTTAG	22	5545	5566	2,499	12
MDV1-M11-3p	TGAGTTACATGGTCAGGGGATT	22	5506	5527	264	77
MDV1-M12-5p	AGGCCCTCCGTATAATGTAAAT	22	7706	7727	195	66
MDV1-M12-3p	TTGCATAATACGGAGGGTTCTGT	23	7672	7694	5,136,011	73
	TGCATAATACGGAGGGTTCTGT	22	7672	7693	736,934	10
MDV1-M31-5p	GGCCAGCTCACTGGCTGTGCACT	23	5053	5075	368	68
MDV1-M31-3p	TGCTACAGTCGTGAGCAGATCAA	23	5016	5038	25,188	30
	TGCTACAGTCGTGAGCAGATC	21	5018	5038	19,551	23
	TGCTACAGTCGTGAGCAGATCA	22	5017	5038	16,728	20

[a] List of MDV-1 miRNAs detected by deep sequencing showing their prevalence as well as all the viral miRNA isoforms that contribute ≥10% of the total reads for that miRNA.

clusters, PARalyzer predicted 1,104 cellular mRNAs that were bound by one or more MDV-1 miRNAs, while 1,183 cellular mRNAs were predicted to be bound by one or more MDV-2 miRNAs. The lack of correlation between the relative abundance of the MDV-1 and MDV-2 miRNAs (Fig. 1A) and the number of miRNA binding clusters, while to some extent unexpected, has nevertheless also been observed in previous efforts to define miRNA target sites using CLIP (36). Of these viral miRNA binding clusters, 419 (~38%) were predicted to be targeted by both MDV-1- and MDV-2-encoded miRNAs (Fig. 2B). Of note, PARalyzer also predicted that MDV-1 miR-M3-5p, miR-M7-5p, and miR-M12-3p, as well as MDV-2 miR-M14-5p, miR-M18-5p, miR-M24-3p, and miR-M28-5p, all of which exist in two isoforms differing at their 5′ ends (Tables 1 and 2 and Fig. 2C) bind to two overlapping but distinct sets of mRNA targets in MSB1 cells, due to their two different seed sequences. Whether the ability of these miRNAs to extend their mRNA targetome by generating two distinct miRNA 5′ isoforms is important for MDV-1 and/or MDV-2 replication is not currently known.

Viral mRNA targets of MDV-1 and MDV-2 miRNAs. Analysis of miRNA binding clusters on the MDV-1 genome identified five very strong binding clusters between positions ~7200 and ~7800, near the 5′ end of the MDV-1 genome (Fig. 3A). These clusters essentially coincide with, but are antisense to, the highly expressed MDV-1 miRNAs miR-M2, miR-M3, miR-M4, and miR-M12, which are adjacent to each other and all located antisense to an MDV-1 mRNA that encodes the viral RLORF8 protein (Fig. 3A). Similarly, we also detected very strong binding clusters near the 5′ end of the MDV-2 genome, coincident with, but antisense to, the MDV-2 miRNAs miR-M24, miR-M28, and miR-M29. Again, these are located antisense to an MDV-2 gene, in this case RLORF2 (Fig. 3B). Previously, we have reported that miRNAs encoded by HSV-1 that are located antisense to the viral immediate early protein ICP0 or the late viral protein ICP34.5 not only give rise to readily detectable miRNA binding clusters on the cognate viral mRNA species in infected cells but also inhibit ICP0 and ICP34.5 expression (8, 37). We therefore wished to determine whether the four MDV-1 miRNAs expressed antisense to RLORF8

TABLE 2 MDV-2 miRNAs expressed in MSB-1 cells[a]

miRNA	Sequence	Length	Position Beginning	End	Frequency	%
MDV2-M14-5p	GTGTGGTACGGTGCACCCTGAGA	23	6911	6933	85,064	31
	TGTGGTACGGTGCACCCTGAGA	22	6911	6932	84,422	31
MDV2-M14-3p	TCAGGAAGTTCCGTGCCCGAA	21	6876	6896	7,775	37
MDV2-M15-5p	TGGAAGGGAAAGGCAAACCGGA	22	6683	6703	3,270	71
MDV2-M15-3p	TGTGTTTTTCCCTTCCATCGCA	22	6640	6661	343,988	71
MDV2-M16-5p	ATCCAGTCTGTTTTGGCATCTGA	23	5547	5569	1,323,176	73
MDV2-M16-3p	AGATGCCAGAGAGACTGAAAT	21	5507	5527	430	41
MDV2-M17-5p	AGTCCTTCCCGGGTCCCCTAGA	22	5160	5181	183,305	76
MDV2-M17-3p	TAGGACAACCGGGACGGACAGG	22	5126	5147	201,610	66
MDV2-M18-5p	GTTTTCTCTCAGGCTGGCATTGC	23	5001	5023	214,786	31
	GTTTTCTCTCAGGCTGGCATTGCA	24	5000	5023	150,712	22
	TGTTTTCTCTCAGGCTGGCATTGC	24	5001	5024	99,695	14
MDV2-M18-3p	CAATGCCTGCGGAGAGAAAGA	21	4961	4981	10,011	70
MDV2-M19-5p	CCCCTCGGCGGTGTGCACGGG	21	4844	4864	1,267	53
	CCCCTCGGCGGTGTGCACGG	20	4845	4864	408	17
	CCCCTCGGCGGTGTGCACGGGT	22	4844	4865	349	14
	CCCCTCGGCGGTGTGCACGGGA	22	4843	4864	249	10
MDV2-M19-3p	CATGCCCCCTCCGAGGGTAGC	22	4804	4825	353	85
MDV2-M20-5p	TCCTTAGCGTGGTGCCTGAGA	21	4694	4714	555,354	73
	TCCTTAGCGTGGTGCCTGAG	20	4696	4715	77,179	10
MDV2-M20-3p	TCAAGTACTGCGCGCAAGGACCG	23	4654	4676	101,333	52
MDV2-M21-5p	TCCTCCTTCGCGGGGTGCTTGA	22	4559	4580	175,317	74
MDV2-M21-3p	GAGCACCACGCCGATGGACGGAG	23	4517	4539	9,299	28
MDV2-M22-5p	TCTTACACGCACGTCACTCTGGT	23	4279	4301	314,713	49
	TCTTACACGCACGTCACTCTGGTC	24	4278	4301	200,784	32
MDV2-M22-3p	AGTGGCTTGCTTGTAGGCTGT	21	4243	4263	12,183	22
MDV2-M23-5p	ATGGTCCGTGGTACGGTGTCCT	22	4130	4151	2,266	54
MDV2-M23-3p	GTCTCCGTACACCGGACCATCG	22	4094	4115	2,975	48
MDV2-M24-5p	TTTTTCCCTTACGGTGCCTGACG	23	3539	3561	96,126	75
MDV2-M24-3p	TTAGATGCCGTCAGGGAAAGAT	22	3503	3524	202,003	62
	TAGATGCCGTCAGGGAAAGATG	22	3502	3523	42,917	13
MDV2-M25-5p	CCTCCTTCGGACGAGTGCTTGCC	23	3391	3413	430	24
	CCTCCTTCGGACGAGTGCTTGC	22	3391	3412	412	23
	CCTCCTTCGGACGAGTGCTTGCCG	24	3391	3414	383	21
	TCCTTCGGACGAGTGCTTGCCG	22	3393	3414	237	13
MDV2-M25-3p	TGCACTACTCCGGGGGTAGGAC	22	3353	3374	291	24
MDV2-M26-5p	TCCTTTGTGCTGTGTGTGAGA	21	3258	3278	49,552	78
MDV2-M26-3p	TCGGGCACCGCACCGAAGGATG	22	3221	3243	8,940	36
	TCGGGCACCGCACCGAAGGATGT	23	3221	3243	3,992	16
	TCGGGCACCGCACCGAAGGAT	21	3223	3243	3,531	14
	TCGGGCACCGCACCGAAGGATT	22	3222	3243	3,480	14
MDV2-M27-5p	CTTCGTCCGGTGTTCGAGGCG	21	3121	3141	50,748	67
	CTTCGTCCGGTGTTCGAGGCGT	22	3120	3141	15,467	20
MDV2-M27-3p	CGTCGAGCACCGTGCTGGAGGA	22	3080	3101	46,233	62
	CGTCGAGCACCGTGCTGGAGGAA	23	3079	3101	13,163	18
MDV2-M28-5p	TTCTCGACGCCTACCCTCGGC	21	2901	2921	489,862	36
	TTTTCTCGACGCCTACCCTCGGC	23	2901	2923	226,111	16
	TTCTCGACGCCTACCCTCGGCG	22	2900	2921	182,831	13
	TTTTCTCGACGCCTACCCTCGG	22	2902	2923	151,642	11
MDV2-M28-3p	CCGAGGGTAGGCGCAGAGGA	20	2870	2889	1,242	20
MDV2-M29-5p	TCTTCACGTACCTCTCTATGGC	22	2758	2779	4,704,329	72
MDV2-M29-3p	CATAGTGAGGTACGTGTAGG	20	2724	2743	1,522	42
MDV2-M30-5p	CAACACTCCCTCGGACGCAGCA	22	160933	160954	372,131	58
	CAACACTCCCTCGGACGCAGC	21	160934	160954	152,551	24
MDV2-M30-3p	CTGACGTGCGAGGGAGTGCTCG	22	160897	160918	1,808	67
MDV2-M32-5p	ATTCCATCCTTCGACTAGCGACT	23	5387	5409	415	94
MDV2-M32-3p	TAATAGCCGGACGACGGAGTCT	22	5353	5374	23,910	91

[a] As in Table 1, but showing all observed MDV-2 miRNAs and their isoforms.

are, in fact, able to repress RLORF8 expression. For this purpose, we generated an indicator construct containing the entire RLORF8 open reading frame and 445 bp of the 3′ UTR, encompassing all four predicted MDV-1 miRNA binding sites (Fig. 3A), inserted 3′ to the firefly luciferase indicator gene (*fluc*), as well as expression vectors encoding MDV-1 miR-M2, miR-M3, miR-M4, or miR-M12. Analogous vectors containing two perfect artificial target sites for each miRNA inserted 3′ to *fluc* served as positive
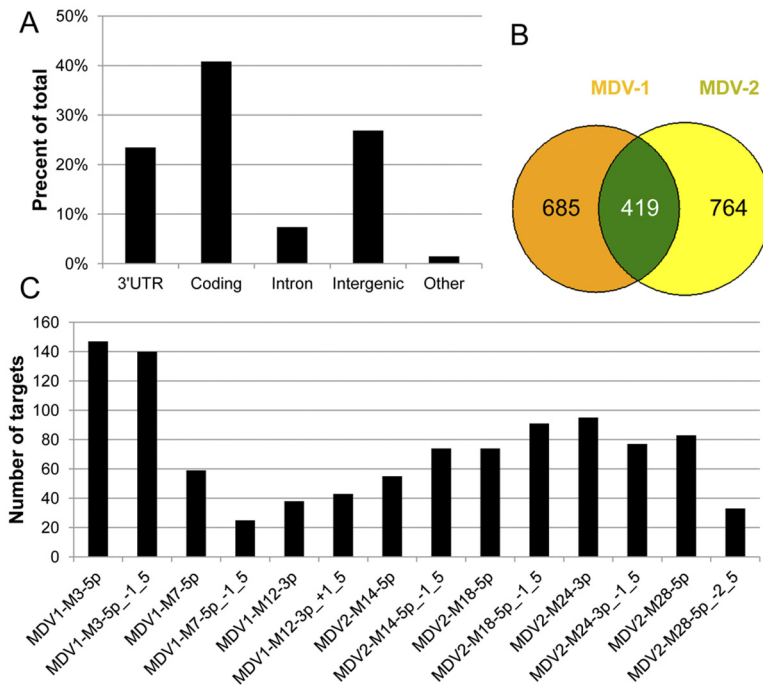
FIG 2 Characterization of the MSB1 PAR-CLIP Library. (A) Annotation of PAR-CLIP clusters that align to a miRNA seed in terms of their genomic origin. (B) Overlapping cellular mRNA targets (coding region plus 3′ UTR plus 500-bp extension) of the MDV-1 and MDV-2 miRNAs. (C) Number of predicted mRNA targets of viral miRNAs that show 5′-end variation and hence have two different seeds.

controls. Finally, we also generated derivatives in which each predicted RLORF8 mRNA target site was mutated in the seed complement. As may be observed in Fig. 4A, cotransfection of each MDV-1 miRNA expression vector into 293T cells along with the positive-control indicator vectors resulted in a clear inhibition in FLuc expression, relative to a cotransfected *Renilla* luciferase (RLuc) internal control vector. Comparison of each wild-type or mutant vector containing the MDV-1 RLORF8 gene sequence showed significant down regulation of the *fluc* vectors containing the wild-type RLORF8 sequence by all four MDV-1 miRNAs. This inhibition was partially (miR-M2 and miR-M4) or totally (miR-M3 and miR-M12) rescued by mutation of each single antisense RLORF8 miRNA target site. These data are consistent with the hypothesis that MDV-1 mRNAs encoding RLORF8 are indeed targets for repression by some or all of these viral miRNAs.

We next generated derivatives of the above-described indicator construct, containing *fluc* linked to the RLORF8 open reading frame and 3′ UTR, that bore seed mutations in all four antisense MDV-1 RNA targets or only in the two targets present in either the RLORF8 open reading frame or the 3′ UTR and transduced these into MSB1 cells, or MDV-negative DT40 cells as a control. As shown in Fig. 4B, the indicator construct bearing mutations in all four of the hypothetical target sites for MDV miR-M2, -M3, -M4, and -M12, gave rise to significantly higher levels of FLuc expression than did the wild-type *fluc* vector, while the indicators containing mutations in only the target sites for miR-M2 and miR-M4 in the RLORF8 ORF or miR-M3 and miR-M12 in the RLORF8 3′ UTR gave intermediate phenotypes. These data again strongly suggest that RLORF8 mRNAs are bona fide targets for repression by MDV-1-encoded miRNAs and indicate that physiological levels of these viral miRNAs, expressed in MDV-1-infected cells, are sufficient to repress RLORF8 mRNA expression.

The finding that expression of the MDV-1 RLORF8 gene product is subject to suppression by as many as four different viral miRNAs suggests that RLORF8 has the potential to reduce MDV-1 replication and/or induce toxicity when expressed inappropriately. To test this hypothesis, we generated a Tet-inducible lentiviral expression vector encoding the RLORF8 open reading frame with both potential internal MDV-1 miRNA target sites mutated and used this to transduce MSB1 cells. After selection for antibiotic resistance, we then added doxycycline (Dox) to induce RLORF8 expression and compared the growth phenotype of MSB1 cells expressing ectopic RLORF8 with that of control cells transduced with a similar lentiviral vector expressing green fluorescent protein (GFP). As may be observed in Fig. 4C, MSB1 cells expressing ectopic RLORF8 indeed grew substantially more slowly than the control cells, consistent with the idea that inappropriate overexpression of RLORF8 can indeed exert a deleterious effect. We have not, however, attempted to determine the molecular basis for this effect, and to our knowledge, the role of RLORF8 in the MDV-1 life cycle remains undetermined.

Ectopic expression of cellular mRNAs targeted by multiple MDV microRNAs. We were intrigued by the apparent ability of ectopic RLORF8, which is targeted by four MDV-1 miRNAs in MSB1, to reduce the growth of MSB1 cells in culture and wondered if other, cellular genes that are targeted by multiple viral miRNAs might exert a similar effect. In Table S2 in the supplemental material, we list 12 cellular genes that are targeted in their 3′ UTRs by five or more MDV-1 or MDV-2 miRNAs, as determined by PAR-CLIP. Of these, two cellular genes, encoding interleukin-18 (IL-18) and CD200R1, are predicted to be targeted by up to seven MDV-1 or MDV-2 miRNAs. IL-18 is a proinflammatory cytokine that can stimulate gamma interferon (IFN-γ) production in T cells (38–40), while CD200R1 is a cell surface
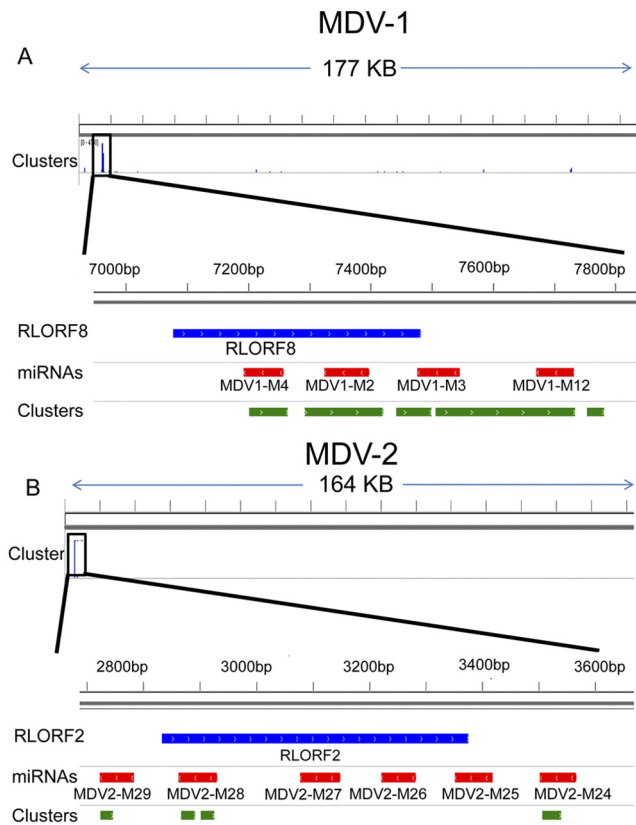
FIG 3 Map of RISC binding clusters that align to the MDV-1 (A) or MDV-2 (B) genome. The size of the peaks is proportional to the read depth of the clusters. A closeup of a 5′ fragment of the MDV-1 and MDV-2 genome that contains the most reads is presented. Open reading frames located on the viral plus strand are marked in blue, viral miRNAs encoded on the minus strand are marked in red, and the approximate location of relevant miRNA binding clusters, identified by PAR-CLIP, is indicated in green.

glycoprotein generally expressed on myeloid cells (41) that has been proposed to play a role in the response to viral infection (42). Of these two genes, the IL-18 gene seemed most likely to exert an antiviral effect in culture, and this mRNA's 3′ UTR was predicted to be targeted by two MDV-1 miRNAs (miR-M2-3p and miR-M9-5p) and as many as five MDV-2 miRNAs (miR-M18-5p, miR-M-18-5p-1_5′, miR-M26-5p, miR-M28-5p, and miR-M30-3p). We therefore generated Tet-inducible lentiviral vectors containing either the chicken IL-18 open reading frame or the IL-18 open frame linked to its cognate 3′ UTR, including all the predicted MDV miRNA target sites. These vectors, plus a control GFP-expressing lentivector, were transduced into MSB1 cells, and puromycin-resistant transductants were selected. These were then analyzed for their growth potential in the presence and absence of Dox (Fig. 5). As may be observed, the control transduced cells grew most rapidly, even in the presence of Dox. Cells transduced with the lentiviral vector containing the IL-18 gene linked to its 3′ UTR grew at a level comparable to that of the control in the absence of Dox but showed a significant reduction in replication in the presence of Dox. Interestingly, even in the absence of Dox, cells transduced with the chicken IL-18 expression vector lacking the IL-18 3′ UTR, and hence all five MDV miRNA target sites, clearly grew more slowly than the controls, thus suggesting that

this inducible expression vector is "leaky" and expresses a low level of IL-18 even in the absence of added Dox. As one would predict, this inhibitory effect became even more severe in the presence of Dox (Fig. 5). Therefore, these data indicate that ectopic expression of chicken IL-18 reduces the replication of MSB1 cells and that this effect is greatly ameliorated if the IL-18 mRNA 3′ UTR, which is detected as a target for several MDV miRNAs by PAR-CLIP, is present in the introduced IL-18 expression vector.

Conserved mRNA targets for miR-155 seed family microR-NAs. As discussed above, MDV-1 encodes a miRNA, miR-M4, that shares full seed homology not only to human and chicken miR-155 but also to the KSHV miRNA miR-K11 (Fig. 6A). Although the role of miR-K11 in transformation of B cells by KSHV remains unclear, it is known that B-cell transformation by EBV, which does not encode a miR-155 analog, is dependent on viral induction of high levels of cellular miR-155 expression (26). Finally, transformation of T cells by MDV-1 has been reported to require miR-M4 function (27). As these miR-155 seed family members all appear to play a key role in herpesviral transformation of lymphoid cells, we reasoned that we might be able to gain important insights into the underlying mechanism by identifying mRNA targets of miR-155, miR-K11, and miR-M4 that are evolutionarily conserved from chickens to humans.

A comparison of mRNA targets for miR-155, miR-K11, and miR-M4, identified by previously reported PAR-CLIP analysis of KSHV-transformed or EBV-transformed human B cells and here for MDV-1 miR-M4 in the MSB1 lymphoblastoid cell line, showed that 9 mRNA targets were detected in all three cell settings, while 4 additional mRNA targets were also conserved in both MDV-1-infected MSB1 cells and EBV-transformed lymphoblastoid cell lines (LCLs) (Fig. 6B) (see Table S3 in the supplemental material for a full listing of mRNA targets for miR-M4 in MSB1 cells). We therefore cloned the 3′ UTRs of all nine mRNAs targeted by all three of these miR-155 seed family members as well as one additional mRNA, encoding JARID2, that is conserved between miR-155 in LCLs and miR-M4 in MSB1 cells but not in PELs. These 3′ UTRs were inserted 3′ to *fluc* and cotransfected into MSB1 cells along with an internal control RLuc vector. In 8 out of 10 cases, we also generated mutant derivatives of these 3′ UTRs in which the predicted MDV-1 miR-M4 target or targets (JARID2 has two predicted miR-M4 targets in its 3′ UTR) were mutated in their region of seed homology. As may be observed, we detected significant and selective repression of FLuc expression mediated by these 3′ UTRs that was partially or entirely alleviated by mutation of the predicted miR-M4/miR-155 target sites. Therefore, although these data did not reveal a statistically significant decline in response to miR-M4 and/or miR-155 expression in all cases, they are consistent with the hypothesis that targeting of the 3′ UTRs of these genes by miR-155 seed family members is conserved between humans and chickens, an evolutionary distance of ~300 million years.

DISCUSSION

The goal of this study was to perform an analysis of the mRNA targetomes regulated by miRNAs encoded by the oncogenic avian herpesvirus MDV-1, and its nonpathogenic relation MDV-2, and in particular to identify mRNAs targeted by MDV miR-M4, which has previously been shown to play a key role in the initiation of T-cell transformation in MDV-1 infected chickens (27). Our interest in miR-M4 was prompted by the previous observation that
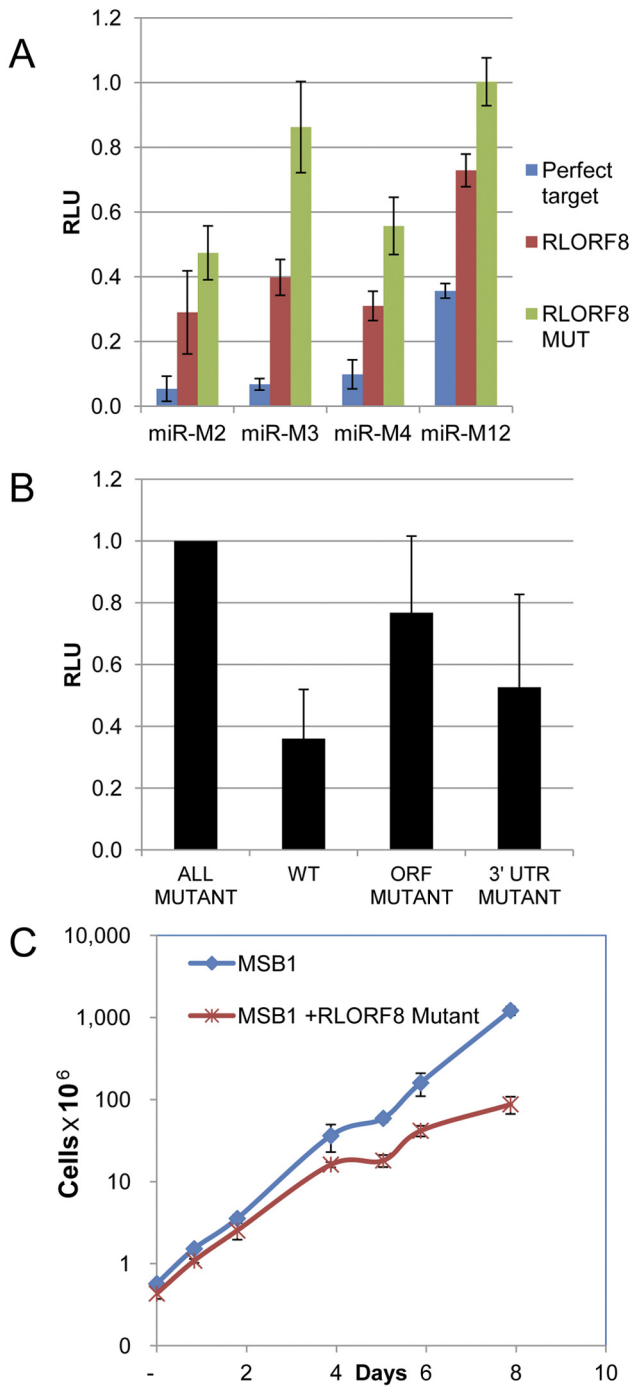
FIG 4 RLORF8 expression is regulated by MDV-1 miRNAs. (A) RLORF8 and its 3′ UTR were cloned downstream of the *fluc* reporter gene. The level of the FLuc indicator was then measured after cotransfection into 293T cells together with the indicated MDV-1 miRNA expression vector. The FLuc-to-RLuc ratios observed for each indicator vector and miRNA were normalized to the ratio in cells that were transfected with the pLCE vector without miRNA. The values obtained in cells expressing only FLuc without a 3′ UTR were set at 100%. The error bars indicate standard deviations (SD) (*n* = 3). (B) We constructed *fluc*-based lentiviral vectors in which *fluc* was linked to the wild-type RLORF8 ORF and 3′ UTR, derivatives in which the MDV-1 miRNA targets in the ORF (miR-M4 and miR-M2) or 3′ UTR (miR-M3 and miR-M12) were mutated, or finally a derivative (ALL MUTANT) in which all four RLORF8 miRNA target sites were mutated. After transduction into MSB1 cells and DT40 cells, the FLuc expression ratio of MSB1 to DT40 cells was determined,
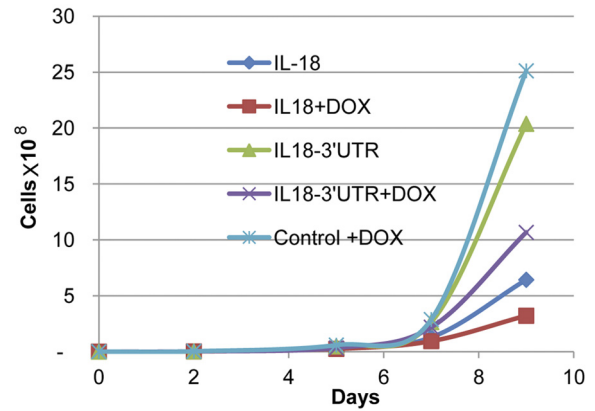
(Continued)

FIG 5 Ectopic expression of chicken IL-18 inhibits the growth of MSB1 cells. MSB1 cells were transduced with Dox-inducible lentiviral expression vectors that express the IL-18 gene with or without its cognate 3′ UTR under the control of a Tet-inducible promoter. Transduced cells were selected using puromycin for 2 weeks, and cell growth was analyzed starting 5 days after Dox addition. The graph is representative of three independent experiments.

miR-M4 shows full seed homology with both the KSHV-encoded miRNA miR-K11 and with miR-155 (19–21), a cellular miRNA that is highly conserved from birds to mammals (Fig. 6A). As discussed above, it seems highly probable that KSHV miR-K11 and human miR-155 play a key role in B-cell transformation mediated by KSHV and EBV, respectively, and, given the high conservation of miR-155 across vertebrate evolution, we therefore hypothesized that the identification of mRNA targets that are targeted by not only miR-K11 and miR-155 in human B cells but also miR-M4 in chicken lymphoblastoid cells might identify a small set of mRNAs that might play a particularly important role in lymphoid transformation by these diverse herpesviruses.

As a first step in this project, we used deep sequencing to define the viral miRNAs expressed in the chicken lymphoblastoid cell line MSB1, which is naturally infected with both MDV-1 and MDV-2. Our analysis did not identify any novel viral pre-miRNAs beyond the 13 previously identified in MDV-1 and the 18 identified in MDV-2 (14–18). We did, however, demonstrate that several MDV-1 and MDV-2 miRNAs exist in two isoforms differing by 1 or 2 nt at their 5′ ends (Tables 1 and 2 and Fig. 1C). These viral miRNAs therefore exist in two isoforms with two different seed sequences that are predicted to target overlapping but distinct populations of mRNA transcripts. Our subsequent PAR-CLIP analysis of the mRNAs targeted by the MDV-1 and MDV-2 miRNAs expressed in MSB1 cells indicated that this was indeed the case (Fig. 2C).

PAR-CLIP identified a list of 1,104 cellular mRNAs targeted by MDV-1 miRNAs and a list of 1,183 mRNAs targeted by MDV-2 miRNAs in MSB1, of which 419 mRNA targets were shared (Fig. 2B). This is reminiscent of our previous analysis of a human PEL cell line coinfected by KSHV and EBV, which identified an

Figure Legend Continued

and this is presented relative to the value for the "ALL MUTANTS" clone, which was set at 1.0. Data are averages for three independent samples with SD. (C) Induced expression of a mutated RLORF8 open reading frame lacking MDV-1 miRNA binding sites inhibits MSB1 growth. Data are averages from five independent experiments with SD.
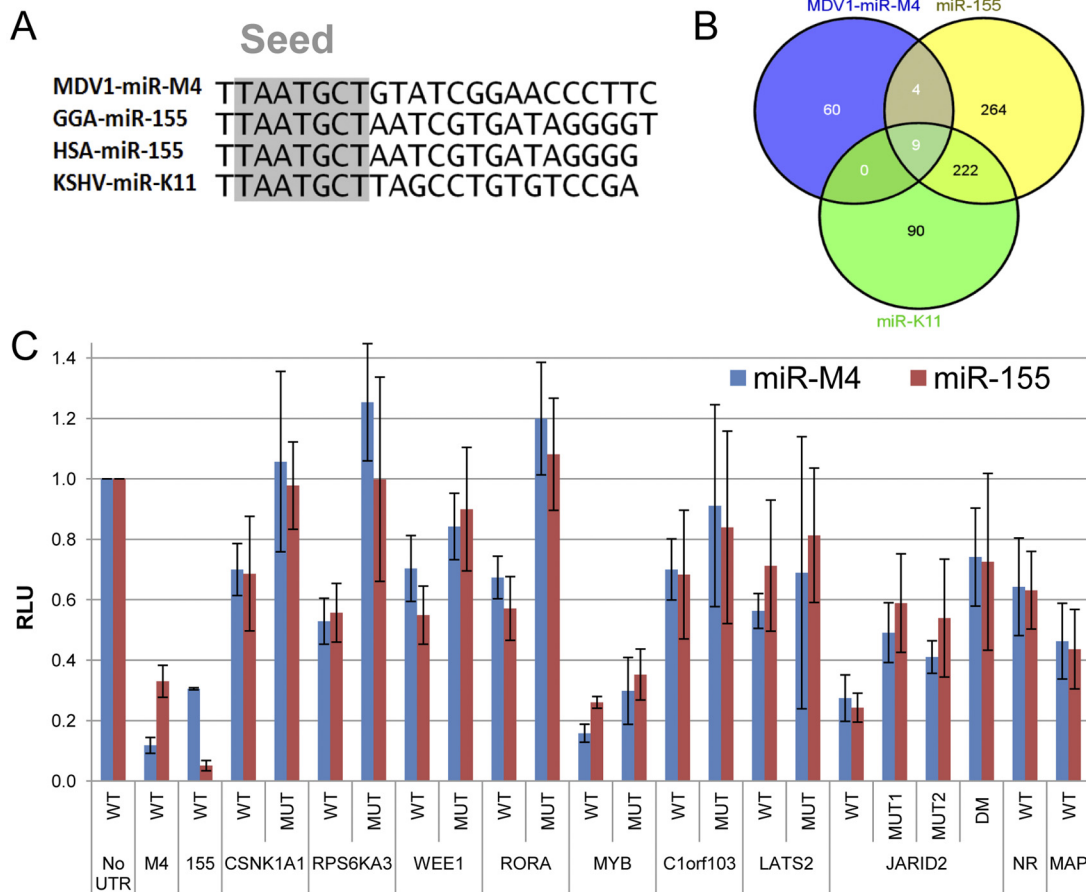
FIG 6 Conserved cellular mRNA targets of miR-M4. (A) MDV1 miR-M4 seed homology with human and chicken miR-155 and KSHV miR-K11. (B) Venn diagram of overlapping targets of miR-M4, miR-155, and KSHV miR-K11. (C) Luciferase reporter assay. 3′ UTRs of genes predicted to be targeted by MDV-1 miR-M4 were cloned with or without mutation of the predicted M4 target site into the 3′ UTR of an *fluc* indicator plasmid. This plasmid, together with an RLuc internal control and the relevant miRNA expression vector, was then cotransfected into 293T cells. The FLuc-to-RLuc ratios observed for each indicator vector and miRNA were normalized to the ratio in cells that were transfected with pLCE without miRNA. The values obtained with cells expressing only FLuc without 3′ UTR were set at 100%. The error bars indicate SD ($n = 3$).

extensive overlap between the cellular mRNA species targeted by EBV and KSHV miRNAs, even though these viral miRNAs lack any significant homology (28). This suggests that herpesviruses that target the same cell type have undergone convergent evolution leading to the expression of distinct viral miRNAs that nevertheless target overlapping sets of cellular factors via different 3′ UTR target sites.

Given the very large number of mRNA targets identified by PAR-CLIP analysis of the MDV-1 and MDV-2 miRNA targetome (see Table S1 in the supplemental material), we have as yet performed only a limited validation and phenotypic analysis of these targets. One mRNA target that was validated is the MDV-1 mRNA encoding the viral RLORF8 protein, which lies antisense to no fewer than four MDV-1 miRNAs in the MDV-1 genome. As predicted by this location, we observed the most intense RISC binding clusters detected on the MDV-1 genome at the location of the RLORF8 transcript (Fig. 3A) and analysis of indicator constructs in cotransfected 293T cells (Fig. 4A) or transduced MSB1 cells (Fig. 4B) confirmed that RLORF8 is indeed targeted by all four of these MDV-1 miRNAs. Interestingly, expression of the MDV-1 RLORF8 gene in a form lacking the viral miRNA binding sites

caused a substantial reduction in MSB1 cell growth (Fig. 4C), consistent with the idea that dysregulated expression of RLORF8 can exert a deleterious effect in MDV-1-infected T cells. However, the function of RLORF8 in the viral life cycle is currently unknown, and we do not yet know why overexpression inhibits the growth of MDV-infected cells. The same pattern is observed in MDV-2, where five viral miRNAs are transcribed from the DNA strand located antisense to RLORF2 (Fig. 3B). Of note, the RLORF2 and RLORF8 proteins do not share significant amino acid sequence homology, and we were also unable to detect any significant homology between these two MDV proteins and proteins encoded by other herpesvirus species. Nevertheless, it remains possible that MDV-1 RLORF8 and MDV-2 RLORF2 do have similar functions. Targeting of MDV-1 genes by MDV-1-encoded miRNAs is not restricted to miRNAs transcribed from the antisense strand, as MDV1-M7-5p was previously shown to downregulate the MDV-1 immediate early genes ICP-4 and ICP-27 (43). Interestingly, in the human α-herpesvirus HSV-1, viral miRNAs are transcribed antisense to ICP0, a viral immediate-early gene, and ICP34.5, a late gene, and downregulate the expression of these genes (8, 37). Although the physiological

relevance of the regulation of viral transcripts by viral miRNAs is not currently clear, it is possible that downregulation of viral early genes helps to maintain the latent phase, while the targeting of the late genes contributes to maintaining the regulated expression of immediate early, early, and late genes upon lytic infection.

Analysis of cellular mRNAs targeted by MDV-1 and/or MDV-2 mRNAs identified several that were targeted by five or more different viral miRNAs in their 3′ UTRs (see Table S2 in the supplemental material), suggestive of a possibly important role in restricting innate antiviral immunity. One factor that is expressed from an mRNA containing as many as seven viral miRNA target sites in its 3′ UTR is the chicken IL-18 gene. IL-18 is a proinflammatory cytokine that is induced upon infection by several different viruses and stimulates IFN-γ production from T cells (40). As the MSB1 cell line is of T-cell origin, we were interested in whether ectopic expression of IL-18 would indeed result in reduced cell growth. In fact, MSB1 cell growth proved to be highly sensitive to inhibition by ectopic IL-18 expression, though it remains to be determined whether this is indeed due to induction of chicken IFN-γ expression (Fig. 5). Thus, our data expose a second way in which MDV manipulates the host cell immune response, in addition to expressing a viral interleukin-8 (vIL-8) protein that is required for disease progression and tumor development (44, 45).

As noted above, we were particularly interested in identifying chicken mRNAs targeted by MDV-1 miR-M4, and PAR-CLIP indeed resulted in the identification of 73 mRNA 3′ UTR targets for miR-M4, of which 9 had previously been identified as targets for miR-155 or KSHV miR-K11 in EBV-transformed human B cells and KSHV-transformed human B cells, respectively (see Table S3 in the supplemental material). Indicator analysis of these 3′ UTRs, several of which have previously been validated as miR-K11 or miR-155 targets, gave data consistent with the hypothesis that these mRNAs are indeed targets for both miR-M4 in MSB1 and miR-155 in human B-cell lymphomas. Particularly interesting shared gene targets for miR-155/miR-M4/miR-K11 include JARID2, a histone methyltransferase and a known target for miR-155 in avian cells that has been shown to promote apoptosis and decrease cell survival when ectopically expressed (46), and LATS (large tumor suppressor), a protein kinase component of the Hippo pathway that inhibits YAP transcriptional activity and therefore both inhibits cell proliferation and promotes apoptosis. LATS sequence and function is evolutionarily conserved from avians to mammals and its loss is observed in many human cancers, including acute lymphoblastic leukemia (47). These activities suggest a potential selective advantage for MDV-1 in inducing downregulation of LATS. Another interesting miR-155/miR-M4/miR-K11 target, NF-κB-inducing kinase (MAP3K14/NIK), was reported to be an important regulator of the noncanonical NF-κB pathway (48). NIK is important for the development of both B cells and T cells (49–51) and may also have the potential to inhibit viral replication. It will therefore be of interest to test whether knockdown of these mRNAs using siRNAs can compensate for the previously reported loss of cell growth seen in EBV-transformed human B cells upon inhibition of miR-155 expression (26).

MATERIALS AND METHODS

Small RNA libraries and PAR-CLIP. Small RNA and PAR-CLIP libraries were constructed as previously described (32, 52). A 3-ml MSB1 cell pellet was used for PAR-CLIP, and the RISC pull-down was performed with a pan-Ago antibody (Abcam: AB 57113) that also recognizes chicken Ago proteins (data not shown). The resulting reads were pre-processed using the FASTX-Toolkit (http://hannonlab.cshl.edu/fastx_toolkit/). Reads longer than 15 nt were aligned to the chicken (Gallus_gallus-4.0 ENSEMBLE), MDV-1 (GenBank accession no. AF243438.1) or MDV-2 (GenBank accession no. AB049735.1) genome using Bowtie (53). One mismatch was allowed in the small RNA library alignments and three in the PAR-CLIP library alignments.

For the analysis of PAR-CLIP data, we used PARalyzer version 1.1 (34) with the following parameters: a minimum cluster read depth of 15 and at least 2 T-to-C conversion locations were required. miRNA assignments to each cluster, based on the small RNA libraries, were designated according to standard nomenclature (1) with a minimal seed match of "7mer1A." Human orthologs of chicken genes were assigned based on ENSEMBLE annotation. In order to avoid possible misannotation of the chicken genome, we included in our annotation 500 bp downstream of the predicted 3′ UTR, as detailed in Table S1 in the supplemental material. The data reported in this paper include this extension as part of the 3′ UTR. In order to generate Fig. 3, we used the Integrative Genomics Viewer (IGV) (54, 55).

Cell culture and transduction. MSB1 cells (a gift from Hsiao-Ching Liu) were grown in RPMI 1640 supplemented with penicillin, 10% fetal bovine serum (FBS), 10% tryptose phosphate broth, and 1% sodium pyruvate at 37°C. 293T cells were grown in Dulbecco's modified Eagle medium (Sigma) supplemented with 10% FBS.

Packaging of pGIPZ or pL-CMV-GL3-derived lentiviral vectors was performed in 293T cells using pMDLgpRRE, pRSV-Rev, and pVSV-G (56). pTRIPZ-derived lentiviral vectors were packaged using pCMVΔR8.75 and pMD2G. These plasmids were cotransfected into 293T cells (10-cm plate) using calcium phosphate, and virus was collected after 48 and 72 h to infect 1.5×10^6 MSB1 cells in 6-well plates. Cells were grown for 3 days before selection using puromycin.

Growth curves. Newly transduced MSB1 cells were grown in the presence of puromycin (Sigma) at a final concentration of 1 μg/ml for 14 days to select transductants. Doxycycline (Sigma) at a final concentration of 1 μg/ml was used to induce expression for 3 to 5 days before the initiation of each growth experiment, when MSB1 cells were diluted to 4×10^5 cells/ml. The cells were split into conditioned media several times during the experiment, when the cell concentration exceeded 8×10^5 cells/ml. Cells were counted using FACSCanto and FlowJo software.

Primer extension. Total RNA from 293T cells and MSB1 cells was prepared using TRIzol (Invitrogen). Primer extension was performed using 8 μg of total RNA using an avian myeloblastosis virus primer extension kit (Promega), according to the manufacturer's protocol. Reaction products were analyzed on 15% Tris-borate-EDTA-urea polyacrylamide gels.

Plasmids. DNA fragments containing the pri-miRNA stem-loops of MDV-1 miR-M2, miR-M3, miR-M4, and miR-M12, as well as up to 150 bp of viral genomic flanking sequences, were PCR amplified from total DNA purified from MSB1 cells, using primers listed in Table S4 in the supplemental material. These DNA fragments were then cloned into the previously described pLCE vector (57) using XhoI and EcoRI. For each of the four miRNAs, we cloned two perfect targets into the XhoI and XbaI sites present in the *fluc*-based indicator pL-CMV-GL3 (58) by annealing two long complementary primers (see Table S4). The miR-155 expression plasmid and the indicator plasmid containing perfect targets for miR-155 were described previously (20).

Chicken genes targeted by MDV1 miR-M4 and human miR-155 were cloned into the XhoI and EcoRI sites present in the *fluc* indicator vector pL-CMV-GL3 using primers listed in Table S4 in the supplemental material. These DNA fragments include part of the 500-bp 3′ UTR extension in relevant cases. All forward primers contained an XhoI site, while reverse primers contained an EcoRI site. Primers were chosen using the IDT PrimerQuest website. In order to create mutations in the predicted binding sites of MDV1-miR-M4, the six nucleotides that align to the miR-M4 seed region (nt 2 to 7) in the 3′ UTRs of RORA, RPS, WEE1, CSNK, and

JARID2 were replaced with an Spe1 restriction site (5′ ATCATG 3′). The sequence 5′ CTTA 3′ in the 3′ UTRs of LATS and Orf103 was replaced with 5′ TAGG 3′. The MYB 3′ UTR was cloned twice, first with a 5′ primer starting at the beginning of the 3′ UTR and second with a primer that starts 40 bp downstream of the 3′ UTR start site and does not contain the predicted MDV1 miR-M4 target site.

An ~820 bp DNA fragment containing RLORF8 and its 3′ UTR were cloned into pL-CMV-GL3 using XhoI and EcoRI. Mutations in the predicted miRNA binding sites in the coding and 3′ UTR regions of RLORF8 were generated with primers listed in Table S4 in the supplemental material. These mutations modify part of the seed binding site and part of the region 3′ of the binding site in order to prevent the formation of a stem-loop that may be generated from an internal promoter on the minus strand. The pGIPZ vector used in this study contains GFP instead of RFP and is based on pTRIPZ (Open Biosystems), as previously described (58).

For the growth experiment whose results are shown in Fig. 4C, the RLORF8 open reading frame, including the stop codon, was cloned into pGIPZ in place of *gfp* using AgeI and EcoRI. The introduced mutations in the predicted seed binding sites of MDV-1 miR-M2 and miR-M4 in the RLORF8 ORF preserved the original amino acid sequence. The chicken IL-18 open reading frame was cloned without the 3′ UTR or with the 3′ UTR, including a 500-bp extension, into pGIPZ in place of the *gfp* gene using AgeI and EcoRI.

Luciferase indicator assays. 293T cells were plated in 24-well plates at 10^5 cells per well. Cotransfection of 500 ng of a pLCE-based miRNA expression vector, 20 ng of a pL-CMV-GL3-based *fluc* indicator plasmid and 20 ng of the pL-CMV-Rluc (58) internal control was performed using calcium phosphate. At 72 h posttransfection, cells were lysed in passive lysis buffer, and RLuc and FLuc activities were measured using a dual-luciferase reporter assay system (Promega), according to the manufacturer's instructions. The ratio between the Fluc and internal control Rluc proteins was then determined for each sample. In the experiment whose results are shown in Fig. 4B, MSB1 and DT40 cells were transduced with equal amounts of the pL-CMV-GL3-based lentiviral vector for 72 h prior to analysis.

Sequence data accession number. Sequencing data have been submitted to the NCBI Sequence Read Archive (SRA) (GEO accession number GSE53806). Processed files will be made available upon request.

SUPPLEMENTAL MATERIAL

Supplemental material for this article may be found at http://mbio.asm.org /lookup/suppl/doi:10.1128/mBio.01060-13/-/DCSupplemental.

Table S1, XLSX file, 2.8 MB.
Table S2, XLSX file, 0.1 MB.
Table S3, PDF file, 0.1 MB.
Table S4, PDF file, 0.2 MB.

ACKNOWLEDGMENTS

REFERENCES

1. **Bartel DP.** 2009. MicroRNAs: target recognition and regulatory functions. Cell **136:**215–233. http://dx.doi.org/10.1016/j.cell.2009.01.002.
2. **Cullen BR.** 2004. Transcription and processing of human microRNA precursors. Mol. Cell **16:**861–865. http://dx.doi.org/10.1016/j.molcel.2004.12.002.
3. **Yi R, Qin Y, Macara IG, Cullen BR.** 2003. Exportin-5 mediates the nuclear export of pre-microRNAs and short hairpin RNAs. Genes Dev. **17:**3011–3016. http://dx.doi.org/10.1101/gad.1158803.
4. **Chendrimada TP, Gregory RI, Kumaraswamy E, Norman J, Cooch N, Nishikura K, Shiekhattar R.** 2005. TRBP recruits the Dicer complex to Ago2 for microRNA processing and gene silencing. Nature **436:**740–744. http://dx.doi.org/10.1038/nature03868.
5. **Khvorova A, Reynolds A, Jayasena SD.** 2003. Functional siRNAs and miRNAs exhibit strand bias. Cell **115:**209–216. http://dx.doi.org/10.1016/S0092-8674(03)00801-8.
6. **Cullen BR.** 2013. MicroRNAs as mediators of viral evasion of the immune system. Nat. Immunol. **14:**205–210. http://dx.doi.org/10.1038/ni.2537.
7. **Grundhoff A, Sullivan CS.** 2011. Virus-encoded microRNAs. Virology **411:**325–343. http://dx.doi.org/10.1016/j.virol.2011.01.002.
8. **Umbach JL, Kramer MF, Jurak I, Karnowski HW, Coen DM, Cullen BR.** 2008. MicroRNAs expressed by herpes simplex virus 1 during latent infection regulate viral mRNAs. Nature **454:**780–783. http://dx.doi.org/10.1038/nature07103.
9. **Boss IW, Renne R.** 2011. Viral miRNAs and immune evasion. Biochim. Biophys. Acta **1809:**708–714. http://dx.doi.org/10.1016/j.bbagrm.2011.06.012.
10. **Osterrieder N, Kamil JP, Schumacher D, Tischer BK, Trapp S.** 2006. Marek's disease virus: from miasma to model. Nat. Rev. Microbiol. **4:**283–294. http://dx.doi.org/10.1038/nrmicro1382.
11. **Nair V.** 2005. Evolution of Marek's disease—a paradigm for incessant race between the pathogen and the host. Vet. J. **170:**175–183. http://dx.doi.org/10.1016/j.tvjl.2004.05.009.
12. **Mwangi WN, Smith LP, Baigent SJ, Beal RK, Nair V, Smith AL.** 2011. Clonal structure of rapid-onset MDV-driven CD4+ lymphomas and responding CD8+ T cells. PLoS Pathog. **7:**e1001337. http://dx.doi.org/10.1371/journal.ppat.1001337.
13. **Burnside J, Bernberg E, Anderson A, Lu C, Meyers BC, Green PJ, Jain N, Isaacs G, Morgan RW.** 2006. Marek's disease virus encodes microRNAs that map to meq and the latency-associated transcript. J. Virol. **80:**8778–8786. http://dx.doi.org/10.1128/JVI.00831-06.
14. **Yao Y, Zhao Y, Xu H, Smith LP, Lawrie CH, Sewer A, Zavolan M, Nair V.** 2007. Marek's disease virus type 2 (MDV-2)-encoded microRNAs show no sequence conservation with those encoded by MDV-1. J. Virol. **81:**7164–7170. http://dx.doi.org/10.1128/JVI.00112-07.
15. **Yao Y, Zhao Y, Xu H, Smith LP, Lawrie CH, Watson M, Nair V.** 2008. MicroRNA profile of Marek's disease virus-transformed T-cell line MSB-1: predominance of virus-encoded microRNAs. J. Virol. **82:**4007–4015. http://dx.doi.org/10.1128/JVI.02659-07.
16. **Waidner LA, Morgan RW, Anderson AS, Bernberg EL, Kamboj S, Garcia M, Riblet SM, Ouyang M, Isaacs GK, Markis M, Meyers BC, Green PJ, Burnside J.** 2009. MicroRNAs of gallid and meleagrid herpesviruses show generally conserved genomic locations and are virus-specific. Virology **388:**128–136. http://dx.doi.org/10.1016/j.virol.2009.02.043.
17. **Morgan R, Anderson A, Bernberg E, Kamboj S, Huang E, Lagasse G, Isaacs G, Parcells M, Meyers BC, Green PJ, Burnside J.** 2008. Sequence conservation and differential expression of Marek's disease virus microRNAs. J. Virol. **82:**12213–12220. http://dx.doi.org/10.1128/JVI.01722-08.
18. **Morgan RW, Burnside J.** 2011. Roles of avian herpesvirus microRNAs in infection, latency, and oncogenesis. Biochim. Biophys. Acta **1809:**654–659. http://dx.doi.org/10.1016/j.bbagrm.2011.06.001.
19. **Zhao Y, Yao Y, Xu H, Lambeth L, Smith LP, Kgosana L, Wang X, Nair V.** 2009. A functional microRNA-155 ortholog encoded by the oncogenic Marek's disease virus. J. Virol. **83:**489–492. http://dx.doi.org/10.1128/JVI.01166-08.
20. **Gottwein E, Mukherjee N, Sachse C, Frenzel C, Majoros WH, Chi JT, Braich R, Manoharan M, Soutschek J, Ohler U, Cullen BR.** 2007. A viral microRNA functions as an orthologue of cellular miR-155. Nature **450:**1096–1099. http://dx.doi.org/10.1038/nature05992.
21. **Skalsky RL, Samols MA, Plaisance KB, Boss IW, Riva A, Lopez MC, Baker HV, Renne R.** 2007. Kaposi's sarcoma-associated herpesvirus encodes an ortholog of miR-155. J. Virol. **81:**12836–12845. http://dx.doi.org/10.1128/JVI.01804-07.
22. **Boss IW, Nadeau PE, Abbott JR, Yang Y, Mergia A, Renne R.** 2011. A Kaposi's sarcoma-associated herpesvirus-encoded ortholog of microRNA miR-155 induces human splenic B-cell expansion in NOD/LtSz-scid IL2Rγnull mice. J. Virol. **85:**9877–9886. http://dx.doi.org/10.1128/JVI.05558-11.
23. **Sin SH, Kim YB, Dittmer DP.** 2013. Latency locus complements mi-

croRNA 155 deficiency in vivo. J. Virol. **87**:11908–11911. http://dx.doi.org/10.1128/JVI.01620-13.

24. **Costinean S, Zanesi N, Pekarsky Y, Tili E, Volinia S, Heerema N, Croce CM.** 2006. Pre-B cell proliferation and lymphoblastic leukemia/high-grade lymphoma in E(mu)-miR155 transgenic mice. Proc. Natl. Acad. Sci. U. S. A. **103**:7024–7029. http://dx.doi.org/10.1073/pnas.0602266103.

25. **Cameron JE, Fewell C, Yin Q, McBride J, Wang X, Lin Z, Flemington EK.** 2008. Epstein-Barr virus growth/latency III program alters cellular microRNA expression. Virology **382**:257–266. http://dx.doi.org/10.1016/j.virol.2008.09.018.

26. **Linnstaedt SD, Gottwein E, Skalsky RL, Luftig MA, Cullen BR.** 2010. Virally induced cellular microRNA miR-155 plays a key role in B-cell immortalization by Epstein-Barr virus. J. Virol. **84**:11670–11678. http://dx.doi.org/10.1128/JVI.01248-10.

27. **Zhao Y, Xu H, Yao Y, Smith LP, Kgosana L, Green J, Petherbridge L, Baigent SJ, Nair V.** 2011. Critical role of the virus-encoded microRNA-155 ortholog in the induction of Marek's disease lymphomas. PLoS Pathog. **7**:e1001305. http://dx.doi.org/10.1371/journal.ppat.1001305.

28. **Gottwein E, Corcoran DL, Mukherjee N, Skalsky RL, Hafner M, Nusbaum JD, Shamulailatpam P, Love CL, Dave SS, Tuschl T, Ohler U, Cullen BR.** 2011. Viral microRNA targetome of KSHV-infected primary effusion lymphoma cell lines. Cell Host Microbe **10**:515–526. http://dx.doi.org/10.1016/j.chom.2011.09.012.

29. **Skalsky RL, Corcoran DL, Gottwein E, Frank CL, Kang D, Hafner M, Nusbaum JD, Feederle R, Delecluse HJ, Luftig MA, Tuschl T, Ohler U, Cullen BR.** 2012. The viral and cellular microRNA targetome in lymphoblastoid cell lines. PLoS Pathog. **8**:e1002484. http://dx.doi.org/10.1371/journal.ppat.1002484.

30. **Haecker I, Gay LA, Yang Y, Hu J, Morse AM, McIntyre LM, Renne R.** 2012. Ago HITS-CLIP expands understanding of Kaposi's sarcoma-associated herpesvirus miRNA function in primary effusion lymphomas. PLoS Pathog. **8**:e1002884. http://dx.doi.org/10.1371/journal.ppat.1002884.

31. **Riley KJ, Rabinowitz GS, Yario TA, Luna JM, Darnell RB, Steitz JA.** 2012. EBV and human microRNAs co-target oncogenic and apoptotic viral and human genes during latency. EMBO J. **31**:2207–2221. http://dx.doi.org/10.1038/emboj.2012.63.

32. **Hafner M, Landthaler M, Burger L, Khorshid M, Hausser J, Berninger P, Rothballer A, Ascano M, Jr, Jungkamp AC, Munschauer M, Ulrich A, Wardle GS, Dewell S, Zavolan M, Tuschl T.** 2010. Transcriptome-wide identification of RNA-binding protein and microRNA target sites by PAR-CLIP. Cell **141**:129–141. http://dx.doi.org/10.1016/j.cell.2010.03.009.

33. **Licatalosi DD, Mele A, Fak JJ, Ule J, Kayikci M, Chi SW, Clark TA, Schweitzer AC, Blume JE, Wang X, Darnell JC, Darnell RB.** 2008. HITS-CLIP yields genome-wide insights into brain alternative RNA processing. Nature **456**:464–469. http://dx.doi.org/10.1038/nature07488.

34. **Corcoran DL, Georgiev S, Mukherjee N, Gottwein E, Skalsky RL, Keene JD, Ohler U.** 2011. PARalyzer: definition of RNA binding sites from PAR-CLIP short-read sequence data. Genome Biol. **12**:R79. http://dx.doi.org/10.1186/gb-2011-12-8-r79.

35. **Hirai K, Yamada M, Arao Y, Kato S, Nii S.** 1990. Replicating Marek's disease virus (MDV) serotype 2 DNA with inserted MDV serotype 1 DNA sequences in a Marek's disease lymphoblastoid cell line MSB1-41C. Arch. Virol. **114**:153–165. http://dx.doi.org/10.1007/BF01310745.

36. **Chi SW, Zang JB, Mele A, Darnell RB.** 2009. Argonaute HITS-CLIP decodes microRNA-mRNA interaction maps. Nature **460**:479–486.

37. **Flores O, Nakayama S, Whisnant AW, Javanbakht H, Cullen BR, Bloom DC.** 2013. Mutational inactivation of herpes simplex virus 1 microRNAs identifies viral mRNA targets and reveals phenotypic effects in culture. J. Virol. **87**:6589–6603. http://dx.doi.org/10.1128/JVI.00504-13.

38. **Okamura H, Tsutsi H, Komatsu T, Yutsudo M, Hakura A, Tanimoto T, Torigoe K, Okura T, Nukada Y, Hattori K, et al.** 1995. Cloning of a new cytokine that induces IFN-gamma production by T cells. Nature **378**:88–91. http://dx.doi.org/10.1038/378088a0.

39. **Ghayur T, Banerjee S, Hugunin M, Butler D, Herzog L, Carter A, Quintal L, Sekut L, Talanian R, Paskind M, Wong W, Kamen R, Tracey D, Allen H.** 1997. Caspase-1 processes IFN-gamma-inducing factor and regulates LPS-induced IFN-gamma production. Nature **386**:619–623. http://dx.doi.org/10.1038/386619a0.

40. **Kanneganti TD.** 2010. Central roles of NLRs and inflammasomes in viral infection. Nat. Rev. Immunol. **10**:688–698. http://dx.doi.org/10.1038/nri2851.

41. **Wright GJ, Puklavec MJ, Willis AC, Hoek RM, Sedgwick JD, Brown MH, Barclay AN.** 2000. Lymphoid/neuronal cell surface OX2 glycoprotein recognizes a novel receptor on macrophages implicated in the control of their function. Immunity **13**:233–242. http://dx.doi.org/10.1016/S1074-7613(00)00023-6.

42. **Karnam G, Rygiel TP, Raaben M, Grinwis GC, Coenjaerts FE, Ressing ME, Rottier PJ, de Haan CA, Meyaard L.** 2012. CD200 receptor controls sex-specific TLR7 responses to viral infection. PLoS Pathog. **8**:e1002710. http://dx.doi.org/10.1371/journal.ppat.1002710.

43. **Strassheim S, Stik G, Rasschaert D, Laurent S.** 2012. mdv1-miR-M7-5p, located in the newly identified first intron of the latency-associated transcript of Marek's disease virus, targets the immediate-early genes ICP4 and ICP27. J. Gen. Virol. **93**:1731–1742. http://dx.doi.org/10.1099/vir.0.043109-0.

44. **Engel AT, Selvaraj RK, Kamil JP, Osterrieder N, Kaufer BB.** 2012. Marek's disease viral interleukin-8 promotes lymphoma formation through targeted recruitment of B cells and CD4+ CD25+ T cells. J. Virol. **86**:8536–8545. http://dx.doi.org/10.1128/JVI.00556-12.

45. **Parcells MS, Lin SF, Dienglewicz RL, Majerciak V, Robinson DR, Chen HC, Wu Z, Dubyak GR, Brunovskis P, Hunt HD, Lee LF, Kung HJ.** 2001. Marek's disease virus (MDV) encodes an interleukin-8 homolog (vIL-8): characterization of the vIL-8 protein and a vIL-8 deletion mutant MDV. J. Virol. **75**:5159–5173. http://dx.doi.org/10.1128/JVI.75.11.5159-5173.2001.

46. **Bolisetty MT, Dy G, Tam W, Beemon KL.** 2009. Reticuloendotheliosis virus strain T induces miR-155, which targets JARID2 and promotes cell survival. J. Virol. **83**:12009–12017.

47. **Jiménez-Velasco A, Román-Gómez J, Agirre X, Barrios M, Navarro G, Vázquez I, Prósper F, Torres A, Heiniger A.** 2005. Downregulation of the large tumor suppressor 2 (LATS2/KPM) gene is associated with poor prognosis in acute lymphoblastic leukemia. Leukemia **19**:2347–2350. http://dx.doi.org/10.1038/sj.leu.2403974.

48. **Senftleben U, Cao Y, Xiao G, Greten FR, Krähn G, Bonizzi G, Chen Y, Hu Y, Fong A, Sun SC, Karin M.** 2001. Activation by IKKalpha of a second, evolutionary conserved, NF-kappa B signaling pathway. Science **293**:1495–1499. http://dx.doi.org/10.1126/science.1062677.

49. **Claudio E, Brown K, Park S, Wang H, Siebenlist U.** 2002. BAFF-induced NEMO-independent processing of NF-kappa B2 in maturing B cells. Nat. Immunol. **3**:958–965. http://dx.doi.org/10.1038/ni842.

50. **Yin L, Wu L, Wesche H, Arthur CD, White JM, Goeddel DV, Schreiber RD.** 2001. Defective lymphotoxin-beta receptor-induced NF-kappaB transcriptional activity in NIK-deficient mice. Science **291**:2162–2165. http://dx.doi.org/10.1126/science.1058453.

51. **Rowe AM, Murray SE, Raué HP, Koguchi Y, Slifka MK, Parker DC.** 2013. A cell-intrinsic requirement for NF-κB-inducing kinase in CD4 and CD8 T cell memory. J. Immunol. **191**:3663–3672. http://dx.doi.org/10.4049/jimmunol.1301328.

52. **Umbach JL, Cullen BR.** 2010. In-depth analysis of Kaposi's sarcoma-associated herpesvirus microRNA expression provides insights into the mammalian microRNA-processing machinery. J. Virol. **84**:695–703. http://dx.doi.org/10.1128/JVI.02013-09.

53. **Langmead B, Trapnell C, Pop M, Salzberg SL.** 2009. Ultrafast and memory-efficient alignment of short DNA sequences to the human genome. Genome Biol. **10**:R25. http://dx.doi.org/10.1186/gb-2009-10-3-r25.

54. **Robinson JT, Thorvaldsdóttir H, Winckler W, Guttman M, Lander ES, Getz G, Mesirov JP.** 2011. Integrative genomics viewer. Nat. Biotechnol. **29**:24–26. http://dx.doi.org/10.1038/nbt.1754.

55. **Thorvaldsdóttir H, Robinson JT, Mesirov JP.** 2013. Integrative Genomics viewer (IGV): high-performance genomics data visualization and exploration. Brief. Bioinform. **14**:178–192. http://dx.doi.org/10.1093/bib/bbs017.

56. **Dull T, Zufferey R, Kelly M, Mandel RJ, Nguyen M, Trono D, Naldini L.** 1998. A third-generation lentivirus vector with a conditional packaging system. J. Virol. **72**:8463–8471.

57. **Zhang J, Jima DD, Jacobs C, Fischer R, Gottwein E, Huang G, Lugar PL, Lagoo AS, Rizzieri DA, Friedman DR, Weinberg JB, Lipsky PE, Dave SS.** 2009. Patterns of microRNA expression characterize stages of human B-cell differentiation. Blood **113**:4586–4594. http://dx.doi.org/10.1182/blood-2008-09-178186.

58. **Gottwein E, Cullen BR.** 2010. A human herpesvirus microRNA inhibits p21 expression and attenuates p21-mediated cell cycle arrest. J. Virol. **84**:5229–5237. http://dx.doi.org/10.1128/JVI.00202-10.